Environ Biol Fish (2025) 108:515–532
https://doi.org/10.1007/s10641-024-01656-6

Investigating eye lens composition for stable isotope analysis in fishes: a comparison between Chondrichthyes and Actinopterygii

Jonathon P. Kuntz · Miranda Bell-Tilcock · Julie L. Vecchio · Amy A. Wallace · Anna M. Sturrock · Sean M. Perry · Sora L. Kim

Received: 31 March 2024 / Accepted: 6 December 2024 / Published online: 17 December 2024

Abstract Life history ecology provides a framework for understanding the complex interactions between organisms and their environments but is challenging to resolve for long-lived and migratory species. In fishes, the combination of movement and foraging ecology is predominantly explored with stable isotope analysis (SIA) of accretionary tissues, such as otoliths. An alternative archival tissue validated for SIA in Actinopterygii (i.e., ray-finned fishes) is the proteinaceous eye lens and its growth layers (laminae). Here, we aim to expand the SIA of laminae to include Chondrichthyes (cartilaginous fishes; sharks, skates, rays, sawfish, and chimeras). We observe that urea in the eye lens drives patterns of elemental composition (i.e., C:N ratio) for Chondrichthyes, but the isotopic effect of urea is negligible. Actinopterygian fishes exhibit consistent C:N ratios across eye lenses, while chondrichthyan eye lens laminae C:N ratios decrease from the inner post-apoptotic laminae to outer pre-apoptotic laminae. After confirming the presence of urea in the Leopard Shark (*Triakis semifasciata*) eye lens laminae with attenuated total reflectance (ATR)-Fourier transform infrared (FTIR) spectroscopy and urea assays, we successfully removed urea from eye lens laminae via three deionized water rinses. Subsequently, the C:N ratios of post-urea extracted Leopard Shark eye lens laminae exhibited similar patterns to actinopterygian fishes. Urea removal from Leopard Shark eye lens

Supplementary Information The online version contains supplementary material available at https://doi.org/10.1007/s10641-024-01656-6.

J. P. Kuntz (✉) · S. L. Kim
Department of Life & Environmental Sciences, University of California Merced, 5200 Lake Rd, Merced, CA 95343, USA
e-mail: jonkuntz93@gmail.com

M. Bell-Tilcock
Center for Watershed Sciences, University of California Davis, 1 Shields Ave, Davis, CA 95616, USA

M. Bell-Tilcock
Delta Stewardship Council, 715 P Street, Sacramento, CA 95814, USA

J. L. Vecchio
South Carolina Department of Natural Resources, Marine Resources Research Institute, Charleston, SC 29412, USA

A. A. Wallace
Cooperative Institute for Marine Ecosystem and Resources Studies, Hatfield Marine Science Center, Oregon State University, Newport, OR 97365, USA

A. M. Sturrock
School of Life Sciences, University of Essex, Wivenhoe Park, Colchester CO4 3SQ, UK

S. M. Perry
Mississippi Aquarium, 2100 E Beach Blvd, Gulfport, MS 39501, USA

laminae increased in $\delta^{15}N$ values as expected, but the isotopic effect was within analytical error. Our results indicate the utility of chondrichthyan eye lens laminae as chronological tissues for SIA. However, there are isotopic effects dependent on urea concentrations. This study demonstrates the need for inter-taxa comparison when establishing novel methodologies in SIA.

Keywords Shark · Urea · Lipid · Movement · Diet · Ecology · Biochemistry

Introduction

Habitat use and trophic dynamics vary with ontogeny but are difficult to discern for long-lived, mobile aquatic and marine organisms, such as chondrichthyans (i.e., cartilaginous fishes; sharks, skates, rays, sawfish, and chimeras) and actinopterygians (i.e., ray-finned fishes). Many ecological studies serially sample inert accretionary tissues from fishes (e.g., aragonite otoliths in actinopterygians and cartilaginous vertebrae in chondrichthyans) for stable isotope analysis (SIA), which provides a lifetime record of diet and/or habitat use. However, these inert and primarily inorganic structures are not present across all fishes and prevent comparisons between chondrichthyans and actinopterygians. An alternative inert, accumulative, and proteinaceous tissue is the eye lens and its layers (laminae). Most studies using eye lens laminae for SIA focus on actinopterygian fishes (Wallace et al. 2014; Bell-Tilcock et al. 2020; Vecchio and Peebles 2020), but there is potential for using this archival tissue in chondrichthyans (Quaeck-Davies et al. 2018; Simpson et al. 2019). However, differences in biomolecule levels, such as lipids and urea, can affect SIA and differ among Chondrichthyes and Actinopterygii. For example, chondrichthyans are neutrally buoyant with large, lipid-rich livers and osmoregulate by retaining urea (Hazon et al. 2003; Gleiss et al. 2017), which are different mechanisms than actinopterygian fishes. Thus, it is important to characterize the taxon-specific differences in elemental components of eye lenses to establish chondrichthyan eye lens laminae as a chronological tissue for SIA.

Stable isotope composition ($\delta^{13}C$ and $\delta^{15}N$) can reveal the diet and habitat use of a consumer. The $\delta^{13}C$ and $\delta^{15}N$ values of an individual's tissues are dependent on its nutritional resources, which varies based on the isotopic composition of primary producers, and extent of differentiation with trophic level (DeNiro and Epstein 1978; Post 2002). Isotopic differentiation at each trophic step occurs with physiological processes that sort (i.e., fractionate) and change the isotopic ratio (e.g., $^{13}C/^{12}C$ and $^{15}N/^{14}N$). For example, organisms respire and excrete waste with the expelled CO_2 and N enriched in the light isotope (i.e., ^{12}C and ^{14}N), causing biomagnification of the heavy isotope (i.e., ^{13}C and ^{15}N) in consumer tissues (DeNiro and Epstein 1978; Post 2002). In addition, different consumer tissues uptake stable isotopes at different rates (i.e., incorporation rate; Tieszen et al. 1983; Carleton and Del Rio 2005; Weidel et al. 2011; Kim et al. 2012b) and have different offsets from diet based on a variety of factors (i.e., trophic discrimination factor; Kim et al. 2012a), which are important for ecological interpretations. While most tissues allow for ecological interpretation based on a single point in time (e.g., muscle, liver, etc.), accretionary or accumulative structures, such as otoliths, cartilaginous vertebrae, and eye lens laminae, continually deposit and provide a time series. In actinopterygian fishes, the SIA of eye lens laminae reflects a chronological record of diet and movement from early development until death (Wallace et al. 2014; Quaeck-Davies et al. 2018; Bell-Tilcock et al. 2020; Vecchio and Peebles 2022). However, a key component to resolving spatial and dietary patterns with SIA is ensuring that biomolecular composition does not coincide with isotopic variation.

Proteinaceous tissues are often the preferred substrate for studying diet with SIA, but varying levels of biomolecules synthesized through various metabolic pathways, such as urea, can affect its isotopic composition. Chondrichthyes exhibit higher levels of urea ($C=O(N–H_2)_2$) for osmoregulation, and since this biomolecule has a higher proportion of nitrogen compared to other biomolecules, it leads to a lower C:N ratio than expected for protein (Kim and Koch 2012). During protein metabolism, it is energetically favorable to synthesize urea as a waste byproduct utilizing ^{14}N, while ^{15}N is preferentially retained in biomolecules such as amino acids. Although most organisms excrete this ^{14}N-enriched urea, the retention of urea in Chondrichthyes lowers the overall bulk tissue $\delta^{15}N$ value (Kim and Koch 2012). In stable isotope ecology studies using muscle, the C:N ratio is often used as

an indicator for urea and monitored for its effects on $\delta^{15}N$ values (Kim and Koch 2012). For example, the C:N ratio of pre-urea extracted Leopard Shark (*Triakis semifasciata*) muscle is approximately 2.7, while post-urea extraction, the ratio increases to approximately 3.2, resulting in a 1.7‰ increase in $\delta^{15}N$ values (Kim and Koch 2012). While the removal of urea from chondrichthyan muscle tissue is recommended and widely practiced, its effect on other tissues, such as plasma and red blood cells, shows inconsistent results (Kim and Koch 2012). Furthermore, to date, there remains no documented evidence of urea in the eye lenses of fishes.

The eye lens is a chronological tissue in the vertebrate eye (Fig. 1(A)) that forms laminae, similar to the layers of an onion, across the entire lifetime of the individual (Wallace et al. 2014; Tzadik et al. 2017). After formation of the outermost membrane (i.e., the lens capsule), a layer of cuboidal epithelial cells adjacent and medial to the capsule forms, divides, and differentiates into lens fiber cells, which are primarily composed of crystallin protein (Fig. 1(B–D); Nicol et al. 1989; Berman 1991; Horwitz 2003; Andley 2008). Primary lens fiber cells are laid down during embryonic development (i.e., lens nucleus), while secondary lens fiber cells are stacked laterally to existing lens fiber cells, creating a layering of laminae (Fig. 1(B); Andley 2008). During the transition from epithelial cell to secondary lens fiber cells, living organelles and their corresponding biomolecules are present for cellular function causing a hydrated laminae (i.e., pre-apoptotic laminae; Fig. 1(B); Berman 1991). After a new suite of lens fiber cells are differentiated, previously established secondary lens fiber cells undergo partial apoptosis, removing living organelles and water molecules, leaving behind a rigid, inert, and tightly packed crystallin protein structure (i.e., post-apoptotic laminae; Fig. 1(B, C)). The eye lens can therefore be serially sampled from the most recently differentiated secondary lens fiber cells (e.g., outer laminae representing most recent time) to inner primary lens fiber cells (e.g., core representing embryonic development/early life). While most of the eye lens is easily sampled, there is a transition zone from rigid post-apoptotic laminae to more hydrated pre-apoptotic that are less distinguishable (Fig. 1(B)). Due to the eye lens being non-vascularized, it receives nutrients via diffusion of aqueous humor across the lens capsule (Berman 1991). In chondrichthyans, these outer hydrated pre-apoptotic laminae

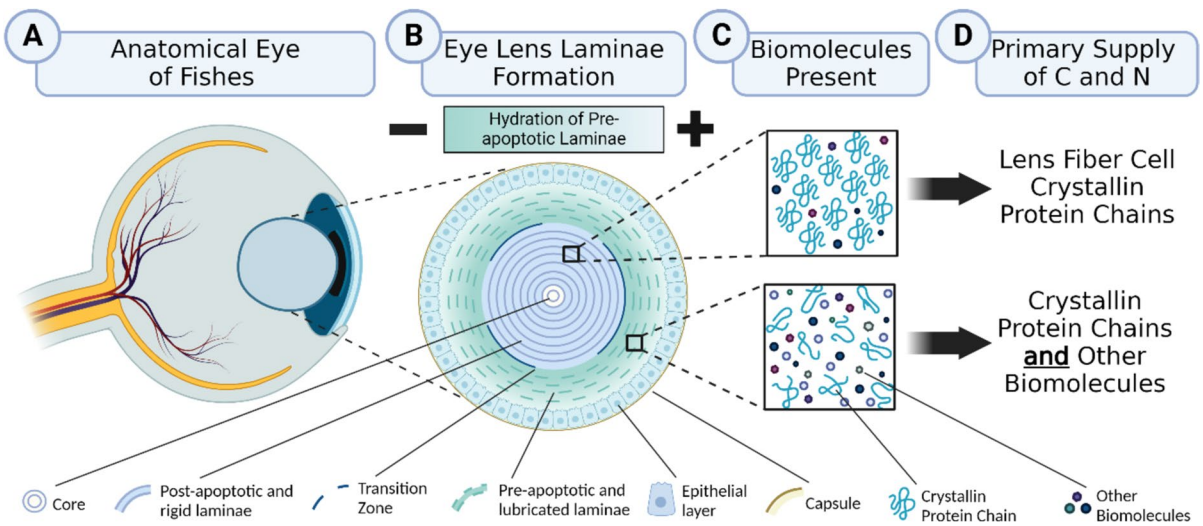

Fig. 1 Diagram of eye lens layer (laminae) formation and possible biomolecular supply of carbon and nitrogen to tissue structure: (A) Generalized anatomical fish eye, with spherical eye lens; (B) eye lens laminae formation with labeled anatomical features from inward to outward (eye lens core, post-apoptotic laminae, pre- and post-apoptotic transition zone, gradient of hydration in pre-apoptotic laminae, epithelial layer, and capsule); (C) labeled biomolecules present in the pre-apoptotic laminae and post-apoptotic laminae (crystallin protein chains and other biomolecules); and (D) primary supply of carbon and nitrogen in the pre-apoptotic laminae (lens fiber cell crystallin protein chains) and post-apoptotic laminae (crystallin protein chains and other biomolecules)

adjacent to the capsule are also permeable (Quaeck-Davies et al. 2018) and may be subject to the addition of uncharacterized biomolecules (Fig. 1(B–D)), such as urea.

The SIA of actinopterygian eye lenses provides crucial insights into patterns of movement and foraging ecology, such as migration, trophic interactions, and natal origin (Wallace et al. 2014; Tzadik et al. 2017; Bell-Tilcock et al. 2020; Vecchio and Peebles 2020, 2022). Few studies have focused on chondrichthyan ecology using eye lens laminae (Quaeck-Davies et al. 2018; Simpson et al. 2019); however, times series of SIA would be particularly useful for ecological studies of ontogeny given their large spatial and temporal ranges. One study to date noted challenges in sampling of outer pre-apoptotic eye lens laminae for chondrichthyans (Quaeck-Davies et al. 2018). The difference in rigid post-apoptotic and hydrated pre-apoptotic laminae was likely representative of a compositional change at the biomolecular scale. While C:N ratio can provide an understanding of large-scale chemical changes, different biomolecular species within a tissue are made up of distinct functional groups. To characterize the biomolecular composition of chondrichthyan eye laminae, we used attenuated total reflectance (ATR)-Fourier transform infrared (FTIR) spectroscopy (Stuart 2004), then quantified changes in urea concentration across eye laminae from post- to pre-apoptotic zones. Here, we ask the following: (1) How do C:N ratios vary across eye lens laminae and among taxa? (2) Is urea presence correlated with changes in C:N ratios of chondrichthyan eye lenses? (3) Does urea affect stable isotope values in the chondrichthyan eye lens? By investigating the chemical and biomolecular makeup of eye lens laminae across Chondrichthyes and Actinopterygii, we aim to establish this substrate to investigate questions regarding movement and foraging ecology across ontogeny.

Materials and methods

Sampling procedures

The biomolecular composition of eye lens was compared between three chondrichthyan species and three actinopterygian species. Our study includes 9 adult Leopard Sharks, 1 adult Sandbar Shark (*Carcharhinus plumbeus*), and 1 adult Zebra Shark (*Stegostoma tigrinum*) for chondrichthyans and 12 juvenile Black Sea Bass (*Centropristis striata*), 12 juvenile Red Grouper (*Epinephelus morio*), and 12 adult Atlantic Salmon (*Salmo salar*) for actinopterygians (Table 1). We dissected and measured eye lens laminae chronologically, offering a means to retroactively reconstruct the life and growth history of an individual fish. Eye lenses were dissected from whole eyes and serially sampled (i.e., delaminated), from the outer lamina, which represented most recent life history, to the laminar core, which represented early development (Fig. 1(B)). For chondrichthyans, serially sampled eye lenses were photographed at × 10 magnification with an imaging camera (Amscope MU1803-HS) attached to stereoscope (Leica S8APO) to later record chronological eye lens laminar measurements. After each lamina was delaminated, we conducted measurements by selecting four evenly spaced directions or angles around the circumference of the eye lens to ensure a representative sampling of measurements for determining its diameter (mm; mean SD = ± 0.1 mm; subset individuals $n = 2$, laminae $n = 31$) via ImageJ (Schneider et al. 2012). The outermost pre-apoptotic laminae, adjacent to the lens capsule, are hydrated

Table 1 List of all species, number of individuals, and locality sampled in this study

Common name	Scientific name	Taxonomic group	Individuals	Locality
Leopard Shark	*Triakis semifasciata*	Chondrichthyes	9	South San Francisco Estuary, CA, USA
Sandbar Shark	*Carcharhinus plumbeus*	Chondrichthyes	1	Captive; Mississippi Aquarium, MS, USA
Zebra Shark	*Stegostoma tigrinum*	Chondrichthyes	1	Captive; Mississippi Aquarium, MS, USA
Black Seabass	*Centropristis striata*	Actinopterygii	12	Eastern Gulf of Mexico, FL, USA
Red Grouper	*Epinephelus morio*	Actinopterygii	12	Eastern Gulf of Mexico, FL, USA
Atlantic Salmon	*Salmo salar*	Actinopterygii	12	Six rivers in the UK—Tweed, North Tyne, Shin, Oykel, Deveron, and Frome

and difficult to measure directly. Consequently, these outermost pre-apoptotic laminae were not included for the Sandbar and Zebra Shark. For the outermost hydrated laminae of the Leopard Sharks, we calculated the laminar midpoint following the method outlined by Vecchio and Peebles (2022). For Actinopterygii, Atlantic Salmon eye lens laminae were also photographed and measured for diameter using an imaging camera (HiChrome HR4K) attached to a stereoscope (Leica S9D), following procedures outlined in Bell-Tilcock et al. (2020). Laminar sampling and manual measuring procedures for Red Grouper and Black Seabass were described in Vecchio and Peebles (2022).

We visually determined the pre- and post-apoptotic transition zones for each individual by recording the diameter of the last rigid post-apoptotic lamina. For species with multiple individuals, such as Leopard Sharks, Black Seabass, and Red Grouper, we estimated the mean pre- and post-apoptotic transition zone. Additionally, we normalized the diameter of each lamina to the capsule diameter for each individual, providing a relative proportion of the eye lens. This normalization allowed for anatomical comparisons both within and across taxa, accommodating fishes with varying eye lens sizes. In the case of Atlantic Salmon, eye lenses were normalized to the last semi-hydrated layer before the outermost hydrated laminae, so no pre- and post-apoptotic transition zone was determined. Eye lens laminae were either desiccated in a drying oven at 55 °C for 12 h or frozen 8 + h and then lyophilized overnight prior to weighing and preparing for SIA at their respective institutions.

Identification of biomolecular compounds

We evaluated the material composition of chondrichthyan eye lenses using ATR-FTIR spectroscopy. In ATR-FTIR, infrared absorption bands identify and quantify organic functional groups and inorganic ions based on reflectance and vibrational movement of chemical bonds (Lee and Chapman 1986). We collected ATR-FTIR spectra of Leopard Shark eye lens laminae (n individuals = 2; n laminae = 29) on a Bruker Vertex 70 Far-Infrared FTIR at the Nuclear Magnetic Resonance Facility of the University of California, Merced. Spectra were collected by smoothing 32 scans per sample from wavelength 400–4000 (cm^{-1}) at a resolution of 4 cm^{-1}. The FTIR spectra of isolated biomolecular compounds serve as a reference to determine individual compounds (Coates 2000; Shurvell 2006), and the size of absorbance of a band in arbitrary units (a.u.) is proportional to the concentration of the associated compound (Grunenwald et al. 2014; Lebon et al. 2016).

Spectra were corrected by flattening expected baseline absorbance bands and fitting smooth spline curves to said baseline bands (Stuart 2004; Trayler et al. 2023). We visually identified absorbance bands in ATR-FTIR spectra and detected each absorbance band's peak (Table 2). To compare shifts in specific absorption band peaks (i.e., amide I and amide II), we normalized each lamina's spectra to the maximum absorption value of the absorption band peak of interest. Additionally, due to the variability in the intensity of absorption band peaks (i.e., max absorbance) in raw FTIR spectra, peak-to-peak ratios are often used to standardize value comparisons between samples (Lebon et al. 2016). Because it was unclear which urea-associated peak-to-peak ratio would be best to indicate urea concentration, we ratioed the urea absorbance band peak (~ wavelength 1449 cm^{-1}) to other individual identified peaks prominent in the spectra (e.g., amide III (1234 cm^{-1}), carboxylate (1392 cm^{-1}), amide II (1516 cm^{-1})) across all laminae. These potential ratios were then compared to the C:N ratio and across the normalized diameter of the eye lens.

Effects of urea extraction

We investigated the impact of urea on stable isotope composition of eye lenses by analyzing samples before and after urea extraction, selecting individual laminae with sufficient material for subsampling (n = 99, across all 9 Leopard Shark individuals). The urea extraction methodology is modified from Kim and Koch (2012) for chondrichthyan muscle. Approximately 1 mg of lamina sample was weighed into a 2-mL microcentrifuge vial, then 1.5 mL of deionized (DI) water was added, and the vial was vortexed for 10 s, sonicated for 30 min, and centrifuged for 3 min. The supernatant was removed using a glass transfer pipette, and this extraction process was repeated 3 × per sample. Because we did not know the urea content of lamina prior to urea extraction and to confirm the efficacy of this method for eye lens laminae,

Table 2 ATR-FTIR absorption bands identified

Functional group	Mean peak wavenumber (cm^{-1})	Literature wavenumber range (cm^{-1})	Description	Citation
Amide III	1234	1200–1350	N–H bending with C–N stretching; C–H and N–H deformation	Singh et al. (1993)
Carboxylate	1392	1310–1410	COO^- symmetric stretch	Parker (1971); Lin et al. (1998); Shurvell (2006)
Urea	1450	1446–1468	Possible N–H bending	Groen and Roberts (2004)
Amide II	1516	1480–1580	C–N stretch coupled to N–H bending; $N–H_3^+$ deformation	Singh et al. (1993); Shurvell (2006)
Amide I	1628	1630–1680	C = O stretch coupled to C–N stretch and N–H bending	Shurvell (2006)
Saturated compounds	2931 and 2966	~2930–2960	Doublet peak: $C–H_2$ stretch and $C–H_3$ antisymmetric stretch	Shurvell (2006)
Secondary amide	3262	3250–3300	Broad band N–H stretch; proteins and polypeptides	Shurvell (2006)

Note: Meak peak wavenumber is the mean wavenumber at maximum absorbance across all laminae. The saturated compound functional group has two linked absorption bands (doublet) in the same region

we analyzed the DI water extract for the outer lamina of three individual Leopard Sharks at two different sample sizes (5 and 10 mg). The DI water used to extract urea for each of the three rinses was transferred to a new microcentrifuge tube and stored at − 20 °C until analysis of urea concentration. The first, second, and third rinses were thawed overnight and individually analyzed at room temperature in triplicate via an EnzyChrom™ urea assay kit III on a 96-well plate BioTek Synergy HTX Multimode Reader at the University of California, Merced. The urea concentrations of the samples (in µM) were determined using a calibration curve ($y = 0.0009x + 0.2818$) based on optical density measurements of urea standard solutions (0 µM, 300 µM, 600 µM, and 1000 µM) for each plate analysis and then converted to ppm. Post-urea extracted laminae samples were frozen, then lyophilized overnight prior to SIA.

Stable isotope analysis

We analyzed eye lens laminae for carbon to nitrogen ratios by weight % (C:N), $\delta^{13}C$ values, and $\delta^{15}N$ values via continuous-flow isotope ratio mass spectrometer coupled to an elemental analyzer (EA-cf-IRMS) via Conflo IV. The $\delta^{13}C$ values are reported relative to Vienna Pee Dee Belemnites (VPDB; ‰), and $\delta^{15}N$ values are reported relative to V-AIR (‰) with values reported as mean ± 1 standard deviation. Leopard Shark, Sandbar Shark, and Zebra Shark laminae were analyzed at the Stable Isotope Ecosystem Laboratory of (SIELO) the University of California, Merced, where data were corrected for linearity and drift using calibrated reference materials (USGS 40 (C:N = 4.28 ± 0.05; $\delta^{13}C = -26.4 \pm 0.1$‰, $\delta^{15}N = -4.5 \pm 0.1$‰, $n = 40$); USGS 41a (C:N = 4.30 ± 0.04, $\delta^{13}C = 36.6 \pm 0.1$‰, $\delta^{15}N = 47.6 \pm 0.1$‰, $n = 22$)) and cross validated using an internal reference material (Mb Squid (C:N = 3.71 ± 0.05, $\delta^{13}C = -18.8 \pm 0.1$‰, $\delta^{15}N = 11.8 \pm 0.1$‰, $n = 14$)). Red Grouper and Black Seabass laminae were analyzed at the University of South Florida College of Marine Science, where NIST 8573 and NIST 8574 L-glutamic acid standard reference materials were used for linearity and drift correction, while analytical precision was obtained using NIST 1577b bovine liver (C:N = 5.63 ± 0.05, $n = 28$). Atlantic Salmon laminae were analyzed at the University of Southampton SEAPORT Stable Isotope Ratio Mass Spectrometry Laboratory, and data were corrected for linearity and drift using calibrated reference materials (USGS 40 (C:N = 4.30 ± 0.07, $n = 26$); USGS 41a (C:N = 4.32 ± 0.04, $n = 25$)).

Statistical analyses

In this study, we performed all statistical analyses in R version 4.3.1 (R Core Team 2023). We determined

the effects of lipids and urea on the chemical composition of eye lens laminae with generalized additive models (GAMs) using the "mgcv" package (Wood 2017). This approach was chosen due to nonlinear relationships between response variables (i.e., C:N ratio, FTIR peak ratio, estimated urea concentration, $\delta^{13}C$ difference, and $\delta^{15}N$ difference) and the two explanatory variables of normalized diameter (smooth term) and fish ID (random smooth effect). GAM assumptions were assessed via the "DHARMa" package (Hartig 2022). In addition, we used a combination of linear regression models (LMs) in the "stats" package (R Core Team 2023) and linear mixed models (LMMs) in the "lme4" package (Bates et al. 2015) to explore data with linear relationships, such as C:N ratio to urea peak-to-peak ratio and C:N ratio to urea concentration. Marginal (fixed effect only) and conditional (fixed and random effect) variance explained (R^2) was calculated for LMMs using the "Mumin" package (Bartoń 2023). We tested assumptions of LMMs via the "DHARMa" package (Hartig 2022) and found that the C:N ratio to urea peak-to-peak ratio models of Urea:Carboxylate, Urea:Amide III, and Urea:Secondary Amide met the assumptions of normality and homoscedacity, whereas the models for Urea:Amide II and Urea:Saturated (both CH_2 and CH_3) did not. The model evaluations of C:N ratio to urea peak-to-peak ratio LMMs used Akaike Information Criterion (AIC) and the likelihood ratio test (LRT) via the "lmerTest" package (Kuznetsova et al. 2017). The Urea:Carboxylate, Urea:Amide III, and Urea:Secondary Amide models exhibited the best AIC scores (Supplemental Table 1). The Urea:Amide II and Urea:Saturated models displayed low AIC scores alongside deviations from normality and homoscedasticity, prompting their exclusion from further analysis. Despite incorporating a random effect to accommodate multiple values per individual (i.e., fish ID), the best C:N ratio to urea peak-to-peak ratio model in terms of AIC included only fixed effects (Supplemental Information Table 1). Consequently, we elected to solely present LM comparison results here (Table 3). Lastly, we used pairwise *t*-tests with a Bonferroni correction in the "stats" package (R Core Team 2023) to compare means of urea concentration between DI water extract sample weight groups (i.e., 5 mg and 10 mg) for each rinse level (i.e., 1, 2, or 3). We also used pairwise *t*-tests to compare means of urea concentration between each combination of rinse pair (i.e., 1 vs 2, 2 vs 3, and 1 vs 3) for each level of DI water extract and sample weight groups (i.e., 5 mg or 10 mg).

Results

Elemental composition across the lens

To our knowledge, there is no inter-taxa comparison of eye lens composition across laminae, which is a critical step in establishing SIA for comparative ecological studies. We observed clear differences in aqueous composition during laminar sampling across the eye lens, delineated by the inner, well-defined laminae (post-apoptotic zone) and the outer, yet-to-be-formed, hydrated laminae (pre-apoptotic zone; see Fig. 1). In addition, there was a gradient of hydration observed for pre-apoptotic laminae from more to less hydration moving from outer to inner laminae (Fig. 1). For Leopard Sharks, the mean transition zone from post-apoptotic to pre-apoptotic occurred at 53% (±4% SD) of the normalized eye diameter (Fig. 2A; dashed line). For Red Grouper and Black Seabass, the mean transition zone occurred at 68% (±8% SD) and 71% (±9% SD) of the eye lens, respectively (Fig. 2B; dashed lines). An accurate transition zone for the Atlantic Salmon eye lens was not calculated due to the data collected during sampling; the normalizing diameter was from the first rigid lamina for each individual rather than total capsule. The transition zone between pre- and post-apoptotic laminae may represent a change in the primary supply of biomolecules across the eye lens (Fig. 1(C, D)).

In this study, we observed a linear and slightly increasing trend in actinopterygian C:N ratios across laminae (no extraction or treatment; Fig. 2B).

Table 3 C:N ratio versus peak-to-peak ratio linear regression model selection

Note: *Akaike Information Criterion (AIC) was used to determine model of best fit

Model	AIC	Edf	R^2	*p* value
C:N ~ peak ratio (Urea:Carboxylate)*	−124.8	27	0.88	<0.001
C:N ~ peak ratio (Urea:Amide III)	−124.2	27	0.88	<0.001
C:N ~ peak ratio (Urea:Secondary Amide)	−80.3	27	0.43	0.001

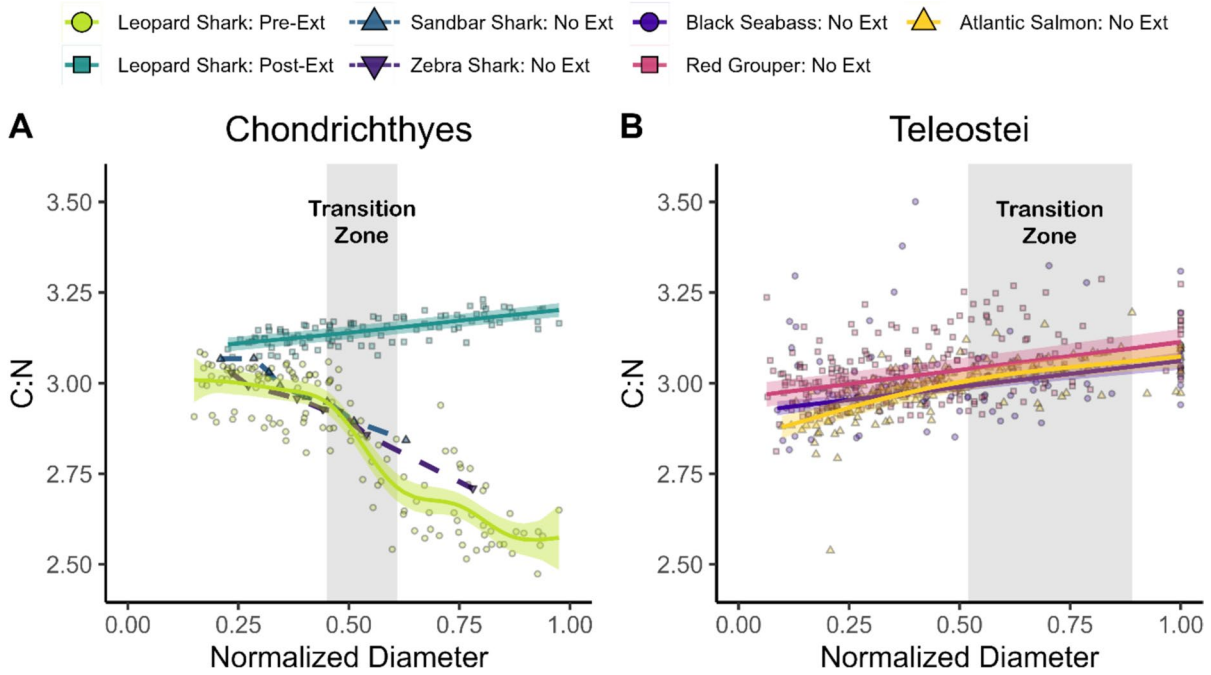

Fig. 2 Carbon to nitrogen ratios (C:N) vary across the normalized diameter of chondrichthyan (**A**) and actinopterygian (**B**) fishes' eye lens laminae. For Leopard Sharks, "Pre-Ext" indicated C:N ratios pre-urea extraction, while "Post-Ext" indicates C:N ratio post-urea extraction. All colored solid lines are GAM smooth mean fit and colored shaded region is the 95% confidence interval around the fit for each species. Dashed lines represent line plots of species with one individual (e.g., Sandbar and Zebra Shark). Grey-shaded region indicates a 95% confidence interval around mean pre- and post-apoptotic transition zone (grey rectangles), Leopard Shark pre-urea extraction (**A**), and min and max for both Black Seabass and Red Grouper (**B**)

Explanatory variables accounted for some of the variance in the response variable (C:N ratio) for Red Grouper and Atlantic Salmon GAMs ($R^2 = 0.65$ and $R^2 = 0.33$, respectively). For both models, the explanatory variables of normalized diameter (smooth term) and fish ID (random smooth effect) were significant ($p < 0.001$ and $p < 0.001$, respectively). For Black Seabass, the explanatory variables explained a low amount of variance in the GAM ($R^2 = 0.04$), where the smooth term of normalized diameter was significant ($p < 0.001$), but fish ID (random smooth effect) was not significant ($p = 0.14$).

Conversely, chondrichthyan C:N ratios in pre-urea extracted laminae exhibited a decreasing trend, notably at the pre- and post-apoptotic transition zone (C:N min = 2.47; max = 3.08; Fig. 2A). A large extent of C:N ratio variance corresponded to explanatory variables in the Leopard Shark pre-extracted GAM ($R^2 = 0.83$; Fig. 2A). The smooth term of normalized diameter was significant ($p < 0.001$), but the random smooth effect of fish ID was not significant ($p = 0.11$). Following urea extractions, Leopard Shark C:N ratios resembled the Actinopterygii trend, with explanatory variables accounting for a greater extent of variance ($R^2 = 0.93$; Fig. 2A). The Leopard Shark post-extracted GAM results indicated significance for both explanatory variables of normalized diameter (smooth term; $p < 0.001$) and fish ID (random smooth effect; $p < 0.001$). These findings highlight distinct patterns in C:N ratios between taxa and effects of urea extraction methods for Chondrichthyes.

ATR-FTIR of eye lens laminae

We identified eight key absorption bands related to amino acids and urea in the ATR-FTIR spectra (Table 2). Each absorption band was exhibited across all laminae (Fig. 3A), but at varying intensities (i.e., peak). We found a shift in the normalized amide I absorption peak to lower wavelengths toward the

outer pre-apoptotic laminae of the eye lens (Fig. 3B). Similarly, we found the formation of a doublet absorption peak for normalized amide II toward the outer pre-apoptotic laminae (Fig. 3C). These subtle changes in the amide I and II functional groups represent structural and biomolecular changes across eye lens laminae.

Peak-to-peak ratios can be an indicator for biomolecular concentration variability within tissues, such as urea levels across eye lens laminae, where the peak ratio of Urea:Carboxylate yielded the lowest AIC value (Table 3). The resulting LM depicted a robust negative linear trend between C:N and Urea:Carboxylate peak ratio ($R^2 = 0.88$, df = 27, $p < 0.001$; Fig. 4A). Informed by these outcomes, we opted to use the Urea:Carboxylate peak ratio in our GAM across the normalized diameter. Our analyses revealed an increase in Urea:Carboxylate absorbance peak ratio following the post- and pre-apoptotic transition zone (Fig. 4B). For the Urea:Carboxylate peak ratio GAM, the explanatory variables accounted for a large portion of the variance ($R^2 = 0.84$), with the smooth term of normalized diameter being statistically significant ($p < 0.001$) and the random smooth effect of fish ID was not significant ($p = 0.411$).

Urea extraction and quantification

Urea contains nitrogen and is known to affect nitrogen isotope composition in chondrichthyan soft tissues;

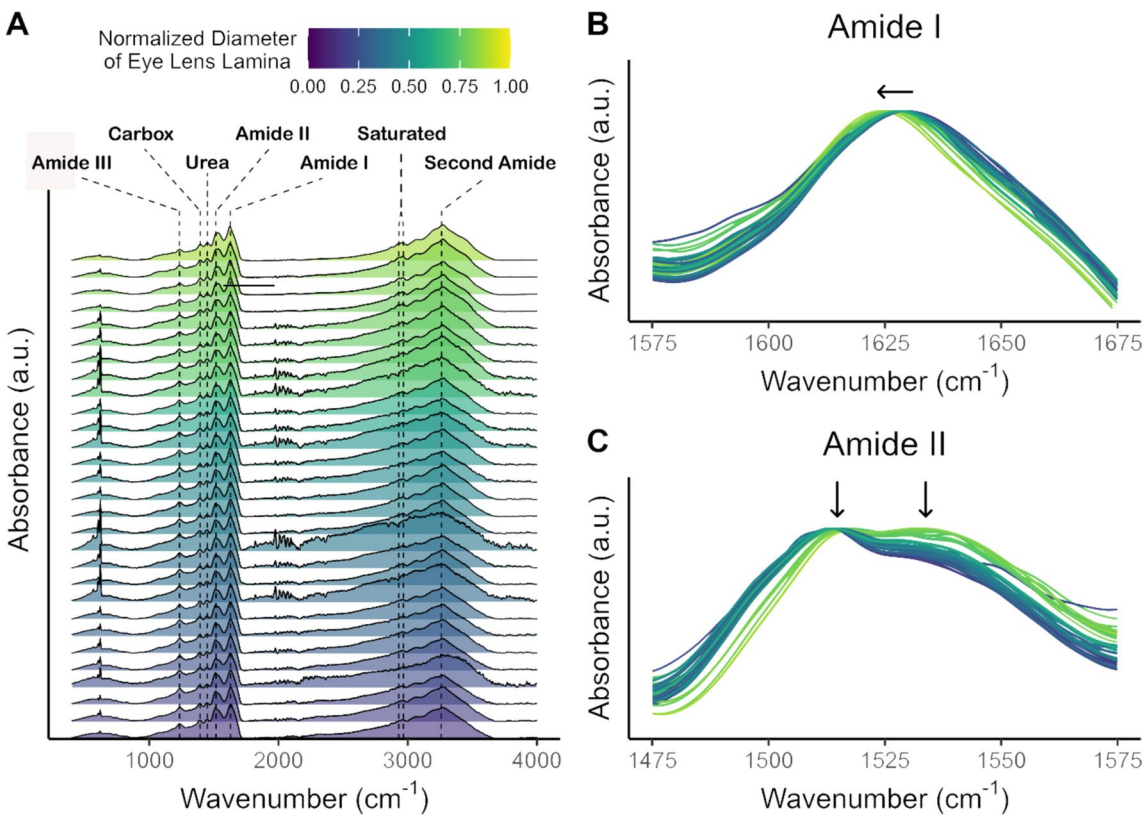

Fig. 3 Amino acid and urea peak absorption bands identified with ATR-FTIR spectra of eye lens laminae from the core (purple) to outer (yellow) laminae. **A** Absorption spectra in arbitrary units (absorption a.u.) across wavelengths (400–4000 cm^{-1}), with dashed vertical line indicating mean wavelength at absorption band peak for all laminae analyzed. **B** Amide I absorption band spectra in arbitrary units (absorption a.u.) across wavelengths (1575–1675 cm^{-1}) normalized to the maximum absorption value of the amide I peak for each lamina, with arrow indicating a shift from higher to lower wavelengths at the amide I peak. **C** Amide II absorption band spectra in arbitrary units (absorption a.u.) across wavelengths (1475–1575 cm^{-1}) normalized to the maximum absorption value of the amide II peak for each lamina, with arrows indicating doublet formation in outer pre-apoptotic laminae. Individual laminae of two Leopard Sharks are represented here

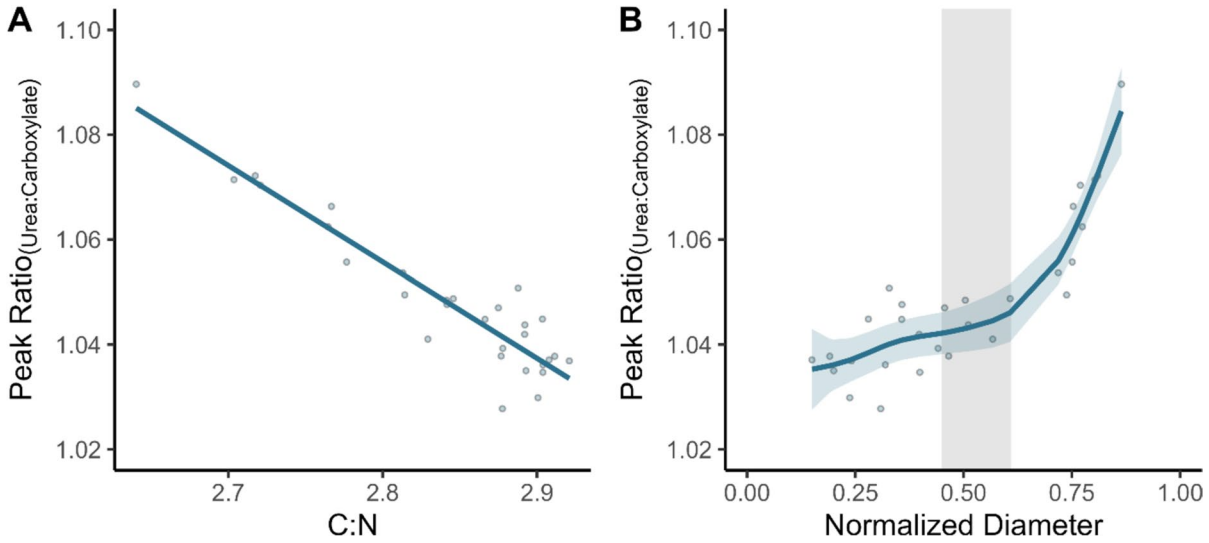

Fig. 4 Leopard Shark laminae ATR-FTIR analyses: **A** Linear regression of the Urea:Carboxylate peak ratio versus carbon to nitrogen ratio (C:N; $R^2 = 0.88$) and **B** GAM smooth curve of the Urea:Carboxylate peak ratio across the normalized diameter of eye lens laminae. The grey-shaded region represents the 95% confidence interval around the pre- and post-apoptotic transition zone

therefore, we quantified urea content to determine possible effects on eye laminae. Urea content was determined from assays on the first, second, and third DI water rinse extract of three individual Leopard Shark outer laminae samples with repetitions at two sample weights. There was no significant difference in pairwise *t*-tests between sample weight groups (i.e., 5 mg versus 10 mg) for rinses 1 and 3 ($p = 0.72$ and $p = 0.61$, respectively), but rinse 2 did indicate a significant mean difference ($p = 0.045$; Fig. 5A). The amount of urea removed with each sequential DI water rinse varied for both sample weights (Fig. 5A). We also found significant differences in means for the 5 mg sample weight group between rinse 1 vs 2 ($p < 0.001$) and rinse 1 vs 3 ($p < 0.001$), but no significant difference between rinse 2 vs 3 ($p = 0.83$; Fig. 5A). Similarly, for the 10-mg sample weight group, we found significant differences in means between rinse 1 vs 2 ($p = 0.02$) and rinse 1 vs 3 ($p = 0.01$), but no significant difference between rinse 2 vs 3 ($p = 0.07$; Fig. 5A).

We used the pre- and post-urea extracted laminae results to correlate urea content and C:N ratio, then estimate urea concentration across the normalized diameter of chondrichthyan eye lenses. There was a linear relationship between urea concentration of DI water rinses (pre-extracted = 1st rinse urea concentration; post-urea extracted = 3rd rinse urea concentration) and C:N ratio (pre- and post-urea extracted eye laminae; Fig. 5B). For the urea concentration (ppm) LMM, the fixed effect (C:N ratio) and random effect (fish ID) explained a high proportion of variance (*marginal* $R^2 = 0.94$; *conditional* $R^2 = 0.96$). The estimated intercept (312.228) and C:N ratio coefficient (−93.728) from the LMM were then used to estimate urea content (ppm) for all Leopard Shark eye lens laminae based on pre-extraction C:N ratio (Fig. 5C). For the estimated urea (ppm) GAM, there was a high amount of variance explained by the response variables ($R^2 = 0.83$) with a significant effect of normalized diameter (smooth term; $p < 0.001$), but no significance of fish ID (random smooth effect; $p = 0.113$). These results are only an estimate and should be interpreted with caution as urea assay concentrations for rinse 1 (5 mg sample mean = 1123.9 ± 155.0 µM; 10 mg sample mean = 1170.3 ± 247.0 µM) fell slightly outside of the range of calibration curve (0–1000 µM) in determining urea concentration.

Urea effect on stable isotopes

We tested if urea presence in eye lens laminae of chondrichthyans affects stable isotope values and

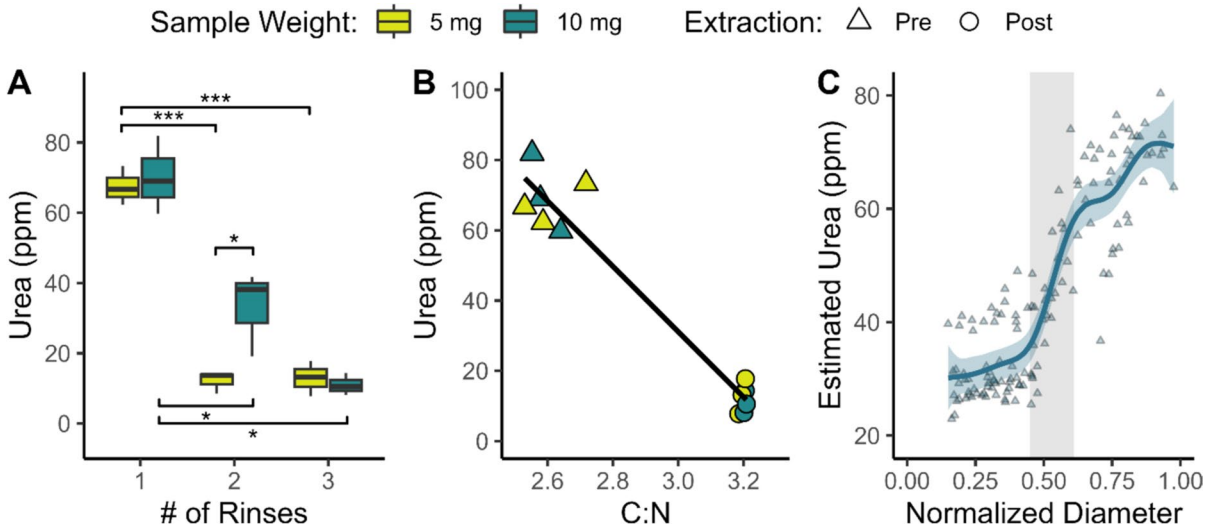

Fig. 5 Boxplots of urea (ppm) in DI water extract post rinse (3×) for different sample weights are shown for the Leopard Shark (**A**). Significant pairwise *t*-tests are denoted with asterisks (i.e., ***$p \leq 0.001$, **$p \leq 0.01$, *$p \leq 0.05$). The linear regression of urea (ppm) versus C:N ratio for pre- and post-urea extracted outer laminae of six individuals is depicted for the Leopard Shark (*B*), with a R^2 value of 0.94. Estimated urea (ppm) GAM mean fit and 95% confidence interval surrounding fit for all pre-urea extracted eye lens laminae across the normalized diameter of the eye lens are shown for the Leopard Shark (**C**). The urea estimates were obtained via the linear mixed model intercept and C:N ratio coefficient from **B**. Grey-shaded region representing the 95% confidence interval around the pre- and post-apoptotic transition zone

found no effects for $\delta^{13}C$ values as well as negligible and/or inconsistent differences for $\delta^{15}N$ values. The $\delta^{13}C$ differences of post-urea extracted minus pre-urea extracted samples resulted in a linear trend near zero, with the GAM fit falling within the 95% confidence interval of $\delta^{13}C$ instrument error (±0.2‰; Fig. 6A). In addition, the explanatory variables for the $\delta^{13}C$ difference GAM accounted for little variance in C:N ratio ($R^2 = 0.03$), and neither the smooth term of normalized diameter and random smooth effect of fish ID had a significant effect ($p = 0.275$ and $p = 0.226$, respectively). The $\delta^{15}N$ difference of post-urea extracted minus pre-urea extracted samples exhibited high variation, but overall increased at the pre- and post-apoptotic transition zone with the GAM fit also falling within the 95% confidence interval of $\delta^{15}N$ instrument error (±0.2‰; Fig. 6B). The $\delta^{15}N$ difference GAM results indicate the explanatory variables accounted for low variance in C:N ratio ($R^2 = 0.03$), similar to the $\delta^{13}C$ difference GAM. The explanatory variables of normalized diameter and random smooth effect of fish ID also did not have a significant effect ($p = 0.079$ and $p = 0.089$, respectively). Although the $\delta^{15}N$ difference GAM fit increases across the post- and pre-apoptotic transition zone, the magnitude of change is muted compared to what is observed without urea extraction (Fig. 6B), and the C:N ratio pattern is similar between actinopterygian eye laminae and chondrichthyan eye laminae after urea extraction.

Discussion

Eye lens laminae are continually synthesized throughout an organism's lifetime, and recent studies analyzed the stable isotope composition of this proteinaceous substrate from fish to elucidate lifetime patterns of diet and movement. Unlike actinopterygian fishes, the body tissues of chondrichthyans contain urea, which has high nitrogen content and can affect $\delta^{15}N$ values (Kim and Koch 2012). Here, we found that patterns of C:N ratios for chondrichthyan eye lens laminae differed from those of several actinopterygian species, with substantially lower C:N ratios in the outer laminae of chondrichthyan eye lenses. Concurrently, we observed a hydrated pre-apoptotic region in Leopard Shark eye lens laminae between the ocular capsule and first rigid laminae (~50% of eye lens diameter) with structural and biochemical differences in the pre- and post-apoptotic zones. Finally,

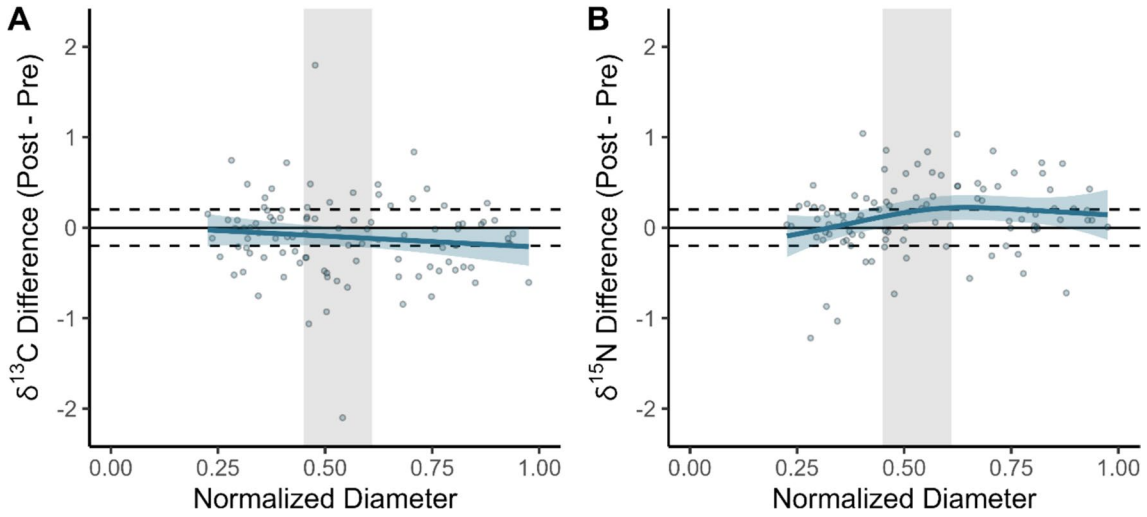

Fig. 6 Leopard Shark GAM smooth curves of **A** $\delta^{13}C$ difference and **B** $\delta^{15}N$ difference (post-extracted minus pre-extracted in both systems) across the normalized diameter of eye lens. Black line indicates zero change, with dashed lines representing 95% confidence interval around average analytical error. Grey-shaded region representing the 95% confidence interval around the pre- and post-apoptotic transition zone

our results indicate that although urea is present, primarily within the pre-apoptotic zone, there is a negligible and inconsistent effect on stable isotope values and DI water rinses minimize potential interference with C:N ratio. These results support the use of eye lenses in fishes as a chronological tissue for SIA, as well as highlighting the potential of chondrichthyan eye lenses in future studies of movement and trophic ecology.

Chondrichthyes C:N patterns differ from actinopterygii

The eye lenses of actinopterygian fishes, across a range of habitats and life history patterns, exhibit remarkably constant C:N ratios. All sampled actinopterygian species demonstrated two distinct sections of the eye lens, a pre-apoptotic and a post-apoptotic section, but the C:N ratios remained relatively consistent from inner to outer laminae (Fig. 2B). This result contrasts sharply with the three chondrichthyan species tested, in which C:N ratio declined precipitously across the diameter, with the most recently formed, outermost layers having the lowest C:N ratios (Fig. 2A).

The content of various organic biomolecules (e.g., amino acids, urea, lipids) affects the elemental and isotopic composition of substrates. For example, lipids have high carbon content from the glycerol group (CH_2OH-$CHOH$-CH_2OH) and fatty acid tails (i.e., carboxylic acid [$-CO_2H$] attached to aliphatic chain [$-CH_3$, $-C_2H_5$, $-C_3H_7$, etc.]). In addition, the metabolic process of lipogenesis (i.e., fatty acid and subsequent triglyceride synthesis) discriminates against ^{13}C, and therefore, lipids are ^{12}C-enriched relative to protein; consequently higher lipid content affects the C:N ratio and $\delta^{13}C$ values of tissue (Post et al. 2007). While lipids make up ~ 2% of the pre-apoptotic portion of the eye lens (by weight) in some fish (Kiss et al. 2010), we did not observe an increase in eye lens laminae C:N ratios greater than $3.87_{\text{weight\%}}$ ($> 3.32_{\text{atomic mass}}$), which is the threshold for lipid effect on $\delta^{13}C$ values (Post et al. 2007). Therefore, lipids are unlikely to be present in high enough concentrations to affect elemental and isotopic composition of the eye lens of fishes.

Originating primarily as a waste byproduct of protein metabolism in the liver, urea serves an additional role in chondrichthyans by aiding in osmotic balance regulation (Hazon et al. 2003). In contrast to the lipid-related increase in C:N ratio, the C:N ratio of proteinaceous tissues decreases with high urea content. This effect stems from urea's high nitrogen content, characterized by two amino groups ($-NH_2$) for every carbonyl group ($-C=O$) (Kim and Koch 2012). Our results show a decreasing C:N ratio across

the normalized diameter of the eye lens in chondrichthyans with a sharp decline near the pre- and post-apoptotic transition zone. This pattern suggests urea presence in the living pre-apoptotic tissue before it undergoes partial apoptosis and subsequent removal of living organelles. In contrast, there was no such change observed in any of the actinopterygian species sampled, regardless of life history strategy (i.e., anadromy). The change in C:N ratio between pre- and post-urea extracted Leopard Shark laminae confirms the removal of some free nitrogenous biomolecular species, which is likely urea. Although urea has not been documented in the eye lenses of any species, its prevalence in shark tissues, including plasma and muscle (Kim and Koch 2012), suggests it may be ubiquitous in soft tissues. Given the likelihood of urea being present in the eye lens laminae of chondrichthyans in concentrations sufficient enough to alter C:N ratios, there is potential for urea to also influence isotopic values.

Structural makeup of chondrichthyes eye lens laminae

The primary component of eye lens laminae is crystallin protein (α or βγ superfamily) with beta-sheet secondary structures (Slingsby et al. 1999). The presence of crystallin protein in the beta-sheet secondary structure of Chondrichthyes eye laminae was confirmed with ATR-FTIR spectroscopy of the amide I absorption band ~ 1630 cm^{-1} (between 1620 and 1640 cm^{-1}; Surewicz et al. 1993; Fatima et al. 2010) and observed throughout the normalized diameter of the Leopard Shark eye lens (Fig. 3A, B). Additionally, the primarily proteinaceous beta-sheet secondary structure was reaffirmed with amide III absorption band ~ 1240 cm^{-1} (Fig. 3A; Singh et al. 1993). The presence of these functional groups confirms the presence of crystallin protein across both pre- and post-apoptotic laminae, including hydrated portions in the pre-apoptotic laminae.

During laminar sampling, we found a distinct difference in degree of hydration between the outer hydrated pre-apoptotic laminae and the inner rigid post-apoptotic laminae. The degree of hydration coincided with a shift in the amide I peak: inner post-apoptotic laminae occurring at higher wavenumbers (~ 1630 cm^{-1}), while outer pre-apoptotic laminae occurring at lower wavenumbers (~ 1620 cm^{-1}; Fig. 3B). This shift in amide I is attributed to changes in protein secondary structure from more complex twisted sheets (longer and fewer strands) to more planar sheets (shorter and more strands; Fatima et al. 2010). In addition, the unfolding of eye lens crystallin proteins from complex and twisted to more planar sheets corresponds with a double, bimodal peak (~ 1517 and 1535 cm^{-1}) in the amide II region of FTIR spectra (Fatima et al. 2010), similar to what we observe in the outer pre-apoptotic laminae (Fig. 3C). While crystallin protein across the eye lens laminae is primarily in the form of beta-sheets, the outer pre-apoptotic laminae likely have a higher proportion of shorter and more planar sheets. These shorter structures may not be able to form compact bonds with adjacent lens fibers, allowing both water molecules and small biomolecules to disperse between the crystallin protein chains. This relationship would explain the correlation between high degree of hydration and changes to C:N ratio in the outer pre-apoptotic laminae.

Beyond the shift in protein secondary structure and interstitial spacing across the eye lens, the change in C:N ratio suggests differences in biomolecular composition. As indicators of compositional shift, absorption band peak-to-peak ratios were coupled with C:N ratios to serve as a proxy for urea concentration within the eye lens. We confirmed urea presence with ATR-FTIR spectroscopy (absorption band peak ~ 1447 cm^{-1}) and observed a significant negative linear relationship between the Urea:Carboxylate peak ratio and C:N ratio (Fig. 4A). The best peak-to-peak ratio model of urea to carboxylate ($-COO^{-}$) normalizes the relative amount of urea to the ionized form of carboxylic acids (-COOH), which is consistently present in amino acids, the primary constituents of crystallin proteins. The peak-to-peak ratio of urea to amide III is similar in terms of AIC and variance explained, likely because of the Amide III peak's association with proteins (Singh et al. 1993). The correlation between the Urea:Carboxylate peak ratio and C:N ratio suggests that higher urea concentrations are associated with lower C:N ratios in eye lens laminae (Fig. 4A). Consequently, we observed an increase in the Urea:Carboxylate peak ratio (i.e., urea concentration proxy) in pre-apoptotic laminae (Fig. 4B), suggesting that higher concentrations of urea are accommodated by the expansion of interstitial spacing across the eye lens. Thus, urea is likely diffused

from the aqueous humor, crossing the capsule, where it accumulates in the pre-apoptotic interstitial space, and the majority of urea is subsequently forced out of the interstitial space as crystallin protein chains become tightly compact during partial apoptosis in the eye lens of Chondrichthyes (Fig. 1(B–D)).

Urea removal and effects on laminae elemental composition

Urea is water soluble and published extraction methods from proteinaceous tissues are relatively straightforward with rinses in DI water. The high C:N ratio and ATR-FTIR results in the outermost laminae confirmed the presence of urea, which we reaffirmed with urea assays of DI water from rinses. The effectiveness of sonication and rinses in DI water to remove urea is attributed to its chemical composition of two amino groups that are hydrophilic. The multiple sonication and rinses with DI water significantly reduced urea concentration in both laminae sample weight groups (i.e., 5 mg and 10 mg) (Fig. 5A). Our results suggest that one rinse is needed to adequately remove urea from chondrichthyan eye lens laminae samples at 5 mg or less, while at least two rinses are needed for 10 mg samples. Because the outermost pre-apoptotic laminae have the highest concentration of urea, post-apoptotic laminae may need less rinses to remove urea.

The concentration of urea likely varies across chondrichthyan eye lens laminae. Although urea assays were only conducted on DI rinses of the outermost pre-apoptotic laminae, we found a strong negative linear relationship between the C:N ratio and the corresponding urea concentration of these laminae (Fig. 5B). Having previously established the correlation between the Urea:Carboxylate peak ratio and C:N ratio (Fig. 4A, B), we can infer the urea concentration (in ppm) for all pre-urea extracted Leopard Shark laminae through the linear relationship: estimated urea (ppm) = 312.228 − [93.728 × C:N ratio] (Fig. 5B). This estimation revealed a doubling in urea concentration from post-apoptotic laminae (~ 30 ppm) to pre-apoptotic laminae (~ 70 ppm; Fig. 5C). We note this pattern may be specific to Leopard Sharks as the urea content within chondrichthyan tissues varies with physiological factors influenced by biological and environmental conditions (Hazon et al. 2003). Pelagic chondrichthyans, such as the Sandbar and Zebra Shark in this study, inhabit more saline environments and often exhibit higher urea concentrations in their tissues to retain water for osmotic balance. In contrast, chondrichthyans inhabiting estuaries, such as Leopard Sharks, may regulate their urea concentration depending on the seasonal or tidal oscillations of salinity (Hazon et al. 2003). However, the Sandbar and Zebra Shark eye lens C:N ratios decreased similarly across the eye diameter compared to the Leopard Shark (Fig. 2A). We suggest additional species should be tested to ensure that the patterns of urea incorporation hold for a wide variety of chondrichthyan taxa, but our results confirm the presence of urea and influence on C:N ratio in chondrichthyan laminae.

Urea levels too small for isotopic effect

High concentrations of urea in chondrichthyan tissues have previously resulted in altered $\delta^{15}N$ values (Kim and Koch 2012). Urea is a waste byproduct enriched in ^{14}N and has lower $\delta^{15}N$ values compared to proteinaceous tissues. In chondrichthyan eye lens laminae, we observed the concentration of urea to differ between pre- and post-apoptotic sections. Urea assays on DI water rinses of Leopard Shark eye lenses indicate urea levels of ~ 30–70 ppm were removed from eye lens laminae, which are high enough to affect C:N ratios; however, the $\delta^{15}N$ difference between post- and pre-urea extracted samples across the normalized diameter was minor and variable, with the model fit falling within the 95% confidence interval of mean analytical error (Fig. 6B). While we observe an increase in the $\delta^{15}N$ difference at the pre- and post-apoptotic transition zone, similar to what we would expect with the removal of urea from pre-apoptotic laminae, the concentration of urea is too low to have a meaningful isotopic effect. Additionally, the $\delta^{13}C$ difference between post- and pre-urea extracted samples across the normalized diameter was also negligible, with the model fit also falling within the 95% confidence interval of mean analytical error (Fig. 6A). It is important to note that although the model fits fell within the 95% confidence interval of analytical error for both $\delta^{13}C$ and $\delta^{15}N$ difference, individual values displayed variability beyond the 95% confidence interval of analytical error for both parameters (Fig. 6A, B). The C:N ratios of post-urea extracted laminae suggest adequate urea removal; however, the high variation and inconsistent directional changes

of stable isotope values suggest the potential loss of other organic biomolecules during extraction. Most of this variation is seen in the pre-apoptotic laminae, where the proteinaceous structure has not yet formed compact and rigid layers; therefore, there is possible loss of free amino acids (i.e., unbound to protein matrix) that would contribute to the variability in urea removal treatment effects. This result aligns with findings by Kim and Koch (2012), who reported similar isotopic variability and effects in plasma and red blood cell samples due to the loss of free amino acids and other organic biomolecules as characterized by gas chromatography mass spectrometry. Therefore, urea removal from chondrichthyan eye lens laminae may have adverse effects on stable isotope values, especially in the pre-apoptotic laminae. This effect may introduce more error into ecological interpretations than the low levels of urea present. Given the effects of urea removal are within analytical error, this step may not be necessary for accurate SIA.

Although the effects of urea on SIA of chondrichthyan tissues are often considered broadly, some species show notable variation in tissue urea concentration, reflecting their unique evolutionary adaptations to osmoregulation (e.g., euryhaline vs stenohaline; Hazon et al. 2003). In this study, our results before and after urea extraction pertain exclusively to Leopard Sharks captured in estuarine waters. Even among captive Leopard Sharks, Kim and Koch (2012) found a high variation in blood urea concentration between individuals, ranging from 400 to 650 mM (~ 24,000–39,000 ppm), which is much higher than the urea levels we found in eye lens laminae, ranging from 7 to 81 ppm. Intra-species variation is further demonstrated in euryhaline individuals; for example, in brackish conditions (50% seawater and 50% freshwater), captive Southern Stingray (*Dasyatis americana*) and Little Skate (*Raja erinacea*) retained only 62.4% and 66.3% of blood urea, respectively, relative to levels in full seawater (Goldstein and Forster 1971; Yancey et al. 1982). Urea is depleted in ^{15}N relative to proteinaceous tissues, and therefore, its presence can influence $\delta^{15}N$ values of whole tissues. Therefore, the higher the concentration of urea in the tissue, the greater its effect on $\delta^{15}N$ values. If the $\delta^{15}N$ values of chondrichthyan urea were known, it would be possible to more accurately predict the threshold at which urea influences the $\delta^{15}N$ values of eye lens laminae using a mass balance approach. However, limitations in extraction methods and the loss of other biomolecules during DI water rinses make isolating urea for post-hoc corrections challenging. While these corrections are difficult to apply, the C:N ratios observed in pre-apoptotic laminae were near the threshold where urea could affect $\delta^{15}N$ values beyond analytical error. Therefore, we recommend performing urea extractions on eye lens laminae with C:N ratios < 2.47, the minimum ratio observed in this study. Additionally, future research should aim to constrain the species-specific effects of urea on stable isotope analysis in chondrichthyan tissues containing free biomolecules, such as pre-apoptotic eye lens laminae.

Conclusion

Eye lens laminae have been validated as a viable tissue type for SIA in Actinopterygii, but our study is the first to examine eye lens laminae series from Chondrichthyes that span post- and pre-apoptotic layers. Our study collected eye lens laminae from three chondrichthyan and three actinopterygian fish species to compare C:N ratio. We showed that the two groups differed in C:N ratio trends across the eye lens. While actinopterygian fishes of varying life histories showed consistent, linear trends in C:N ratio across the eye lens, three species of chondrichthyans showed precipitous declines. We did not observe an indication of lipid effects in eye lens laminae; instead, urea in the chondrichthyan pre-apoptotic portion of the eye lens is likely the cause of differing chemical composition, with intercellular urea responsible for the observed C:N ratios. Although DI water rinses are an effective urea removal method from chondrichthyan eye lens laminae, we did not observe a meaningful isotopic effect in the Leopard Shark, which inhabits estuarine waters. We recommend that future research on chondrichthyan eye lens laminae perform urea extraction only on samples with a C:N ratio below 2.47, as this ensures more accurate $\delta^{15}N$ values for ecological interpretation by minimizing isotopic effects caused by urea. However, for samples with C:N ratios above this threshold, we advise against urea extraction unless improved procedures are developed, due to the minimal isotopic effects observed and the potential unintended removal of other biomolecules. Our findings highlight the

importance of understanding the taxon-specific differences in elemental components of eye lens laminae for confidence in ecological interpretation using SIA.

Acknowledgements We thank those who collected, prepared, and analyzed tissues: Angelique Rea, Evelyn Groom, and Antonio Gonzalez (University of California Merced); Jonny Archer (Tweed River Foundation); Jack Bloomer (Tyne Rivers Trust) and the Environment Agency FBG Team Northeast; Sean Robertson (then Kyle of Sutherland Fisheries); Marcus Walters (Deveron Bogie and Isla Rivers Trust); Rasmus Lauridsen and Luke Scott (Game and Wildlife Conservation Trust); Felix Astejada, Ashmitha Jayachandran Mishma, Michael Bevins Cameron, Lorna McKellar, and Joe Dawson (University of Essex); and Bastian Hambach and Megan Wilding (University of Southampton). We would also like to thank Dr. Robin Trayler (Stable Isotope Ecosystem Laboratory of University of California Merced) for his expertise in SIA and ATR-FTIR spectroscopy, as well as Dr. Rebecca Ryals and Zachary Malone (University of California Merced) for their expertise in biochemical assay techniques. Figure 1 of this publication was created with BioRender.com. JPK salary and analyses funded under NOAA Grant # NA22OAR4170106, California Sea Grant College Program [Project R/HCE-27F], through NOAA'S National Sea Grant College Program, U.S. Dept. of Commerce. AMS salary and analyses funded by a UKRI Future Leaders Fellowship [MR/V023578/1]. The statements, findings, conclusions, and recommendations are those of the author(s) and do not necessarily reflect the views of California Sea Grant, state agencies, NOAA, or the U.S. Dept. of Commerce.

Author contribution Conceptualization: Jonathon P. Kuntz and Sora L. Kim; methodology: Jonathon P. Kuntz, Miranda Bell-Tilcock, Julie L. Vecchio, and Amy A. Wallace; formal analysis and investigation: Jonathon P. Kuntz, Julie L. Vecchio, Anna M. Sturrock; writing—original draft preparation: Jonathon P. Kuntz and Sora L. Kim; writing—review and editing: Jonathon P. Kuntz, Miranda Bell-Tilcock, Julie L. Vecchio, Amy A. Wallace, Anna M. Sturrock, Sean M. Perry, and Sora L. Kim; funding acquisition: Jonathon P. Kuntz, Julie L. Vecchio, Anna M. Sturrock, and Sora L. Kim; resources: Jonathon P. Kuntz, Julie L. Vecchio, Anna M. Sturrock, Sean M. Perry, and Sora L. Kim; supervision: Sora L. Kim.

Funding JPK salary and analyses funded under NOAA Grant # NA22OAR4170106, California Sea Grant College Program [Project R/HCE-27F], through NOAA'S National Sea Grant College Program, U.S. Dept. of Commerce. AMS salary and analyses funded by a UKRI Future Leaders Fellowship [MR/V023578/1].

Data availability Chondrichthyan elemental and isotopic data are available via the open-source, online repository IsoBank (www.isobank.org ID# 872). In addition, attenuated total reflectance (ATR)-Fourier transform infrared (FTIR) spectroscopy data is available via the open-source, online repository Dryad (https://doi.org/10.5061/dryad.mw6m9064k).

Declarations

Ethics approval Leopard Sharks were caught with methods approved by the Institutional Animal Care and Use Committee of the University of California, Merced (protocol # AUP20-0013) and California Department of Fish & Wildlife (permit S-201820001–20182-001). The Sandbar Shark and Zebra Shark ocular tissues were from captive individuals that died of natural causes at the Mississippi Aquarium. Black Seabass and Red Grouper were from the fisheries independent monitoring efforts of the Florida Fish and Wildlife Conservation Commission and the Southeast Area Monitoring and Assessment Program (SEAMAP). Black Seabass and Red Grouper were collected with methods and approval from the Institutional Animal Care and Use Committee of the University of South Florida (Protocol # T IS00003324). Tissues were collected from post-spawned Atlantic Salmon carcasses that had died naturally, approved by the University of Essex Ethics Review and Management System (project ID: ETH2324-0686).

Competing interests The authors declare no competing interests.

References

Andley UP (2008) The lens epithelium: focus on the expression and function of the α-crystallin chaperones. Int J Biochem Cell Biol, 40:317–323. https://www.ncbi.nlm.nih.gov/pmc/articles/PMC3624763/pdf/nihms412728.pdf

Bartoń K (2023) MuMIn: Multi-model inference (1.47.5). The Comprehensive R Archive Network.

Bates D, Machler M, Bolker B, Walker S (2015) Fitting linear mixed-effects models using lme4. J Stat Softw 67:1–48. https://doi.org/10.18637/jss.v067.i01

Bell-Tilcock M, Jeffres CA, Rypel AL, Sommer TR, Katz JVE, Whitman G, Johnson RC (2020) Advancing diet reconstruction in fish eye lenses. Methods Ecol Evol 12:449–457. https://doi.org/10.1111/2041-210X.13543

Berman ER (1991) Biochemistry of the eye. Plenum, New York

Carleton SA, Del Rio CM (2005) The effect of cold-induced increased metabolic rate on the rate of ^{13}C and ^{15}N incorporation in house sparrows (*Passer domesticus*). Oecologia 144:226–232. https://doi.org/10.1007/s00442-005-0066-8

Coates J (2000) Interpretation of infrared spectra, a practical approach. Encyclopedia of Analytical Chemistry. Wiley, Chichester, pp 10815–10837

DeNiro MJ, Epstein S (1978) Influence of diet on the distribution of carbon isotopes in animals. Geochim Cosmochim Acta 42:495–506. https://doi.org/10.1002/mop.25285

Fatima U, Sharma S, Guptasarma P (2010) Structures of differently aggregated and precipitated forms of γB crystallin: an FTIR spectroscopic and EM study. Protein Pept Lett 17:1155–1162. https://doi.org/10.2174/092986610791760414

Gleiss AC, Potvin J, Goldbogen JA (2017) Physical trade-offs shape the evolution of buoyancy control in sharks. Proc R Soc b: Biol Sci 284:20171345. https://doi.org/10.1098/rspb.2017.1345

Goldstein L, Forster RP (1971) Osmoregulation and urea metabolism in the little skate *Raja erinacea*. Am J Physiol 220:742–746. https://doi.org/10.1152/ajplegacy.1971.220.3.742

Groen H, Roberts KJ (2004) An examination of the crystallization of urea from supersaturated aqueous and aqueous-methanol solutions as monitored in-process using ATR FTIR spectroscopy. J Cryst Growth 4:929–936. https://doi.org/10.1021/cg030038y

Grunenwald A, Keyser C, Sautereau AM, Crubézy E, Ludes B, Drouet C (2014) Revisiting carbonate quantification in apatite (bio)minerals: a validated FTIR methodology. J Archaeol Sci 49:134–141. https://doi.org/10.1016/j.jas.2014.05.004

Hartig F (2022) DHARMa: Residual diagnostics for hierarchical (multi-level/mixed) regression models. https://CRAN.R-project.org/package=DHARMa

Hazon N, Wells A, Pillans RD, Good JP, Anderson WG, Franklin CE (2003) Urea based osmoregulation and endocrine control in elasmobranch fish with special reference to euryhalinity. Comp Biochem Physiol B 136:685–700. https://doi.org/10.1016/S1096-4959(03)00280-X

Horwitz J (2003) Alpha-crystallin. Exp Eye Res 76:145–153. https://doi.org/10.1016/S0014-4835(02)00278-6

Kim SL, Koch PL (2012) Methods to collect, preserve, and prepare elasmobranch tissues for stable isotope analysis. Environ Biol Fishes 95:53–63. https://doi.org/10.1007/s10641-011-9860-9

Kim SL, Casper DR, Galván-Magaña F, Ochoa-Díaz R, Hernández-Aguilar SB, Koch PL (2012a) Carbon and nitrogen discrimination factors for elasmobranch soft tissues based on a long-term controlled feeding study. Environ Biol Fishes 95:37–52. https://doi.org/10.1007/s10641-011-9919-7

Kim SL, Del Rio CM, Casper D, Koch PL (2012b) Isotopic incorporation rates for shark tissues from a long-term captive feeding study. J Exp Biol 215:2495–2500. https://doi.org/10.1242/jeb.070656

Kiss AJ, Devries AL, Morgan-Kiss RM (2010) Comparative analysis of crystallins and lipids from the lens of Antarctic toothfish and cow. J Comp Physiol B 180:1019–1032. https://doi.org/10.1007/s00360-010-0475-9

Kuznetsova A, Brockhoff PB, Christensen RHB (2017) lmerTest package: tests in linear mixed effects models. J Stat Softw 82:1–26. https://doi.org/10.18637/jss.v082.i13

Lebon M, Reiche I, Gallet X, Bellot-Gurlet L, Zazzo A (2016) Rapid quantification of bone collagen content by ATR-FTIR spectroscopy. Radiocarbon 58:131–145. https://doi.org/10.1017/RDC.2015.11

Lee DC, Chapman D (1986) Infrared spectroscopic studies of biomembranes and model membranes. Biosci Rep 6:235–256. https://doi.org/10.1007/BF01115153

Lin SY, Li MJ, Liang RC, Lee SM (1998) Non-destructive analysis of the conformational changes in human lens lipid and protein structures of the immature cataracts associated with glaucoma. Spectrochim Acta A 54:1509–1517. https://doi.org/10.1016/S1386-1425(98)00175-9

Nicol J, Colin A, Somiya H (1989) The eyes of fishes. Oxford University Press, Oxford

Parker FS (1971) Applications of infrared spectroscopy in biochemistry, biology, and medicine. Plenum Press, New York. https://doi.org/10.1007/978-1-4684-1872-9

Post DM (2002) Using stable isotopes to estimate trophic position: models, methods, and assumptions. Ecology 83:703–718. https://doi.org/10.1890/0012-9658(2002)083[0703:USITET]2.0.CO;2

Post DM, Layman CA, Arrington DA, Takimoto G, Quattrochi J, Montaña CG (2007) Getting to the fat of the matter: models, methods and assumptions for dealing with lipids in stable isotope analyses. Oecologia 152:179–189. https://doi.org/10.1007/s00442-006-0630-x

Quaeck-Davies K, Bendall VA, MacKenzie KM, Hetherington S, Newton J, Trueman CN (2018) Teleost and elasmobranch eye lenses as a target for life-history stable isotope analyses. PeerJ 6:1–26. https://doi.org/10.7717/peerj.4883

R Core Team (2023) R: A language and environment for statistical computing. https://www.r-project.org/

Schneider CA, Rasband WS, Eliceiri KW (2012) NIH Image to ImageJ: 25 years of image analysis. Nat Methods 9:671–675. https://doi.org/10.1038/nmeth.2089

Shurvell HF (2006) Spectra–structure correlations in the mid- and far-infrared. In: Chalmers JM (Ed) Handbook of Vibrational Spectroscopy. Wiley, Chichester. https://doi.org/10.1002/0470027320.s4101

Simpson SJ, Sims DW, Trueman CN (2019) Ontogenetic trends in resource partitioning and trophic geography of sympatric skates (Rajidae) inferred from stable isotope composition across eye lenses. Mar Ecol Prog Ser 624:103–116. https://doi.org/10.3354/meps13030

Singh BR, Deoliveira DB, Fu F, Fuller MP (1993) Fourier transform infrared analysis of amide III bands of proteins for the secondary structure estimation. Proc SPIE, Biomolecular Spectroscopy III 1890:47–55. https://doi.org/10.1117/12.145242

Slingsby C, Clout NJ (1999) Structure of the Crystallins Eye 13:395–402. https://doi.org/10.1038/eye.1999.113

Stuart BH (2004) Infrared spectroscopy: fundamentals and applications. Wiley, Chichester

Surewicz WK, Mantsch HH, Chapman D (1993) Determination of protein secondary structure by Fourier transform

infrared spectroscopy: a critical assessment. Biochemistry 32:389–394

Tieszen LL, Boutton TW, Tesdahl KG, Slade NA (1983) Fractionation and turnover of stable carbon isotopes in animal tissues: implications for $\delta^{13}C$ analysis of diet. Oecologia 57:32–37. https://doi.org/10.1007/BF00379558

Trayler RB, Landa PV, Kim SL (2023) Evaluating the efficacy of collagen isolation using stable isotope analysis and infrared spectroscopy. J Archaeol Sci 151:105727. https://doi.org/10.1016/j.jas.2023.105727

Tzadik OE, Curtis JS, Granneman JE, Kurth BN, Pusack TJ, Wallace AA, Hollander DJ, Peebles EB, Stallings CD (2017) Chemical archives in fishes beyond otoliths: a review on the use of other body parts as chronological recorders of microchemical constituents for expanding interpretations of environmental, ecological, and life-history changes. Limnol Oceanogr Methods 15:238–263. https://doi.org/10.1002/lom3.10153

Vecchio JL, Peebles EB (2020) Spawning origins and ontogenetic movements for demersal fishes: an approach using eye-lens stable isotopes. Estuar Coast Shelf Sci 246:107047. https://doi.org/10.1016/j.ecss.2020.107047

Vecchio JL, Peebles EB (2022) Lifetime-scale ontogenetic movement and diets of red grouper inferred using a combination of instantaneous and archival methods. Environ Biol Fishes 105:1887–1906. https://doi.org/10.1007/s10641-022-01210-2

Wallace AA, Hollander DJ, Peebles EB (2014) Stable isotopes in fish eye lenses as potential recorders of trophic and geographic history. PLoS ONE 9:e108935. https://doi.org/10.1371/journal.pone.0108935

Weidel BC, Carpenter SR, Kitchell JF, Vander MJ (2011) Rates and components of carbon turnover in fish muscle: Insights from bioenergetics models and a whole-lake ^{13}C addition. Can J Fish Aquat Sci 399:387–399. https://doi.org/10.1139/F10-158

Wood SN (2017) Generalized additive models: an introduction with R. Chapman and Hall/CRC, New York

Yancey PH, Clark ME, Hand SC, Bowlus RD, Somero N, Yancey PH, Clark ME, Hand SC, Bowlus RD, Somero GN (1982) Living with water stress: evolution of osmolyte systems. Science 217:1214–1222. https://doi.org/10.1126/science.7112124